ARTICLE

# Complex Hygrothermal Effects on the Glass Transition of an Epoxy-Amine Thermoset

**Sungwon Choi and Elliot P. Douglas***

Department of Materials Science and Engineering, University of Florida, Gainesville, Florida 32611

**ABSTRACT** Anomalous hygrothermal behavior in an epoxy-amine thermoset was observed in terms of increases in glass-transition temperatures ($T_g$) after immersion in water at different temperatures. Fourier transform near-infrared (FT-NIR) spectroscopic measurements showed that an increase in conversion was responsible for the increase in glass transition, while plasticization occurred simultaneously, rendering the hygrothermal behavior to be complex. To consider other factors affecting this complex hygrothermal behavior, a relationship between $T_g$ and conversion was constructed for the unexposed system and compared to the corresponding $T_g$ values for the exposed system at the same point of each conversion value. With this method, the conversion was successfully excluded to compare the $T_g$ values directly between the unexposed and exposed systems. This indicates the effects of other factors are negligible compared with the large plasticization effect. The plasticization effect was also evaluated quantitatively by observing $T_g$ differences between the unexposed and the exposed system as a function of absorbed water amount estimated by a characteristic water peak in the NIR spectra. The result indicates that there is additional anomalous behavior in which $\Delta T_g$ changes independently of the water amount at higher exposure temperatures.

**KEYWORDS:** epoxy • thermoset • glass transition • cross-link density • hygrothermal effects

## INDRODUCTION

The glass-transition temperature ($T_g$) of a polymer is the temperature at which dramatic changes in properties occur, particularly reduction in strength, stiffness, and resistance to creep. Thus, there is a desire among structural engineers and designers to use the $T_g$ as a materials specification in codes and standards. However, for thermosetting materials used as adhesives and as a component of FRP, such as epoxies and vinyl esters, the glass transition is not a single value. In these materials, the glass transition can vary with factors such as degree of cure and extent of water absorption. These factors are exacerbated by the fact that in civil engineering applications, the material is cured under ambient conditions, and thus is typically not fully cured. Thus, an understanding of how these factors affect the glass transition is of particular importance for defining upper temperature use limits in these applications.

Water absorption into various types of polymer systems has been extensively studied including amorphous (1–4), semicrystalline (5–7), cross-linked polymers (8, 9), and copolymers (10, 11) because of the general tendency of water absorption to induce a loss in physical properties such as a decrease in $T_g$. Plasticization by absorbed water has been generally regarded as the major factor resulting in this property loss.

In epoxy resins, property degradation due to hygrothermal exposure is also a critical issue, in which their nature to absorb moisture up to 7−8 wt % results in a significant loss in $T_g$ (8, 9, 12–20) and modulus (21–25), tensile (23–25), and adhesive strength (26). Plasticization by absorbed water is also considered to be a primary reason to induce property loss, whereas other mechanisms such as hydrolysis and hygrothermal stresses causing swelling, formation of microcracks and crazes, and polymer chain scission may also be factors depending on the material and exposure condition (13, 14, 23–25). The plasticization effect by water has been described from two different viewpoints in terms of epoxy−water interaction (17, 19, 27). From the first view following the concept of polymer−diluent systems, the absorbed water is simply described to reside in the free volume of the network without any interaction between the polymer and water, which enhances the chain mobility, resulting in a structural relaxation transition at lower temperatures (28–30). From another point of view, the water bonds to specific polar groups, such as hydroxyl groups, and disrupts interchain hydrogen bonds, also resulting in a loss in properties (17, 31, 32). In some cases, both effects are considered to occur in the same system (15, 25, 33, 34). In any case, the absorbed water seems to undoubtedly act as a critical stimulus to degrade the properties of epoxy resins. In addition to the presence of absorbed water, the elevated temperature also contributes to the property loss in that the increased rate of water diffusion results in a larger amount of water absorption, whereas chain mobility is also enhanced at higher temperatures.

However, some studies have revealed anomalous behavior, i.e., an increase in physical properties of epoxy systems after hygrothermal exposure, such as an increase in $T_g$ or tensile modulus. Nogueira et al. reported that in an epoxy system, the tensile modulus was slightly increased at certain amounts of water sorption, although it immediately decreased as water content increased (25). They attribute these results to the reactivation of the post-curing reaction. Wu and

* Corresponding author. E-mail: edoug@mse.ufl.edu.
Received for review December 29, 2009 and accepted February 22, 2010
DOI: 10.1021/am9009346



Published on Web 03/02/2010

coworkers also observed anomalous hygrothermal behavior for a nonstoichiometric epoxy system cured at room temperature, in which after 500 days of water immersion at 45 °C, the $T_g$ values and moduli of the specimens with a lower ratio of hardener increased (35). For an epoxy-based primer, Devasahayam also found increases in $T_g$ up to 10 °C for exposure to 95% RH at 55 and 68 °C, whereas almost no change in $T_g$ was found for samples exposed at lower temperatures (36). Other authors have found similar results (37–39), in which an increase of cross-link density by the reactivation of the post-curing reaction is generally attributed as the mechanism for this anomalous behavior.

There have also been other descriptive hypotheses for the anomalous increase in physical properties with hygrothermal exposure. Zhou and Lucas found initial stages of sharp $T_g$ depression followed by significant increases of $T_g$ in three different epoxy resins during hygrothermal exposure (40). Combined with their previous work investigating two types of bound water in epoxy resins through absorption/desorption profiles (27), a theory of different types of hydrogen bonded water was suggested to explain the anomalous behavior. In this theory, single-hydrogen-bonded water acts as a plasticizer, increasing chain mobility and contributing to property loss (Type 1), whereas water molecules interconnected with multiple sites of the resin network through hydrogen bonds create secondary cross-linking, resulting in an increase in physical properties (Type 2). Papanicolaou et al. also employed this model to describe anomalous hygrothermal behavior in an epoxy resin. From dynamic mechanical thermal analysis (DMTA), they found increases in $T_g$ values with decreases in tan $\delta$ values during hygrothermal exposure, whereas storage modulus values showed almost no change (41). They explained this phenomena with the theory of different types of hydrogen bonded water in that Type 1 bound water contributed to the decrease of tan $\delta$ by disrupting initial hydrogen bonds, whereas Type 2 water was responsible for the increase in $T_g$.

It has also been suggested that the biphasic structure in epoxy systems contributes to this anomalous behavior (41). According to this hypothesis, distribution of compression and expansion forces due to differences in water diffusion between hard and soft phases causes an anomalous increase in mechanical properties.

The three suggested mechanisms above for the description of the anomalous behavior of "property gain" under hygrothermal exposure are summarized as follows: (1) post-curing reactions caused by the elevated temperature of the water used for exposure; (2) different states of hydrogen bonded water molecules, one of which creates secondary cross-linking; and (3) effect of biphasic structure. It is important to note, however, that for none of these explanations is there any direct experimental evidence supporting them, and a clear explanation of the mechanism for this anomalous behavior remains unanswered. In this study, we have also observed similar anomalous increases in $T_g$ with hygrothermal exposure. We focus on direct experimental measurements that allow us to specifically describe the mechanism for this behavior.

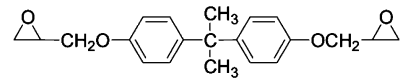

DGEBA

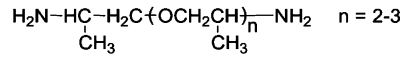

POPDA

**FIGURE 1. Chemical structures of diglycidyl ether of bisphenol A (DGEBA) and poly(oxypropylene)diamine (POPDA).**

**Table 1. Cure and Exposure Conditions for Hygrothermal Exposure**

| type of experiment | cure condition | exposure condition |
|---|---|---|
| changes in $T_g$ using DSC<br>changes in crosslink density using FT-IR | RT/28 days | water immersion at 30, 40, 50, and 60 °C/1, 2, 4, 7, 14, and 28 days |

**Table 2. Cure Conditions for the Master Plot of $T_g$ vs Cross-Link Density for Unexposed Epoxy**

| cure condition | $T_g$ (°C) | epoxide conversion |
|---|---|---|
| RT/0−28days | −56.2−46.8 | 0.00−0.86 |
| 80 °C/110 min | 54.4 | 0.90 |
| 90 °C/80 min | 61.1 | 0.93 |
| 90 °C/110 min | 69.0 | 0.97 |
| 50 °C/60 min + 80 °C/120 min + 125 °C/180 min | 76.7 | 1.00 |

## EXPERIMENTAL SECTION

**Materials.** The material used in this work is a two-part epoxy, diglycidyl ether of bisphenol A (DGEBA) and poly(oxypropylene)diamine (POPDA, Jeffamine D-230), purchased from Huntsman. Figure 1 illustrates the chemical structures of DGEBA and POPDA. The mass ratio of DGEBA to POPDA was 100 to 32.9, corresponding to stoichiometric equivalence between functional groups. The two liquid components were mixed vigorously for 10 min to ensure even mixing. The mixed material was then degassed for 30 mins under vacuum to remove air bubbles. Specimens were cured at room temperature (RT, 22−23°C) for 4 weeks before the exposure was started, ensuring enough time for the curing reaction at RT. Exposure environments consisted of immersion into clean tap water at temperatures of 30, 40, 50, and 60 °C. Details of the cure and exposure conditions for hygrothermal exposure are shown in Table 1.

To construct a master plot of $T_g$ versus cross-link density for the unexposed epoxy, we employed various cure conditions to obtain specimens with a wide range of conversion values. The specific information for cure conditions for these specimens is shown in Table 2.

**Techniques.** Differential scanning calorimetry (DSC; DSC 220, Seiko instruments) was utilized to identify changes in $T_g$ with hygrothermal exposure. Samples were prepared by depositing a small amount of the epoxy formulation directly into the bottom of a DSC aluminum pan before the system was cured in order to maximize the thermal contact between the sample and the pan and avoid the artifacts often observed during first DSC scans when there is poor thermal contact. After the sample was cured in the bottom of the pan either the pan

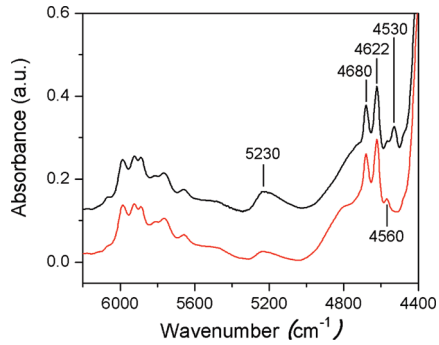


**FIGURE 2. Typical NIR spectra for unexposed systems with different cure conditions: Cured at RT for 28 days (top) and cured at 50 °C for 1 h followed by 80 °C for 2 h and 125 °C for 3 h (bottom).**

with the sample in it was immersed in water for hygrothermal exposure, or the pan was immediately used for $T_g$ measurement. Following hygrothermal exposure, the surface of the sample was wiped carefully with a paper tissue to remove any excess surface water. The pan was immediately sealed and placed directly into the DSC chamber for the measurement. To reduce the potential for any cure occurring during the measurement, we determined the $T_g$ from the first run of each specimen. After placing the sample in the DSC, the heat flow signal was allowed to fully equilibrate before beginning the temperature scan. The temperature range for the measurement was −30 to 130 °C at a heating rate of 10 °C/min, and three replicas were fabricated for each exposure condition to obtain the average value. The $T_g$ was chosen from the midpoint of the tangent between the extrapolated baselines before and after the transition.

To measure cross-link density and the amount of absorbed water, we used Fourier transform infrared spectrometry (FTIR; Nicolet Magna 760, Thermo Electron Cooperation) with a CaF beamsplitter and an MCT detector. Near-infrared spectra were recorded over the range of 3800−7400 $cm^{-1}$ using 32 scans at a resolution of 4 $cm^{-1}$. Thin films with 0.5 mm thickness were cast between glass plates using Teflon spacers. After the selected cure condition as shown in Tables 1 and 2, the films were either immersed in water for hygrothermal exposure or directly used for the FTIR measurement.

Typical NIR spectra for stoichiometric systems without exposure are shown in Figure 2. The reduction in the epoxide absorbance at 4530 $cm^{-1}$ for the higher temperature cure is evident in this figure. For the quantitative analysis of cross-link density changes, the area of the epoxide peak around 4530 $cm^{-1}$ normalized to the phenyl peak around 4622 $cm^{-1}$ was calculated for each exposure condition. The epoxy conversion was then calculated by $\alpha = 1 - A(t)/A(0)$, where $A(t)/A(0)$ is the ratio of normalized peak area with respect to the uncured and unexposed system. For quantitative analysis in accordance with the Beer−Lambert law, the absorbance was less than 1.0. The baselines for area calculation of those peaks were chosen as suggested by Dannernberg without any baseline correction (42). In Figure 2, there is a small unknown peak at around 4560 $cm^{-1}$ that overlaps the epoxide peak. The area of this peak as measured on a stoichiometric, fully cured sample was subtracted from the total area of the peaks in that region in order to determine the absorbance due only to epoxide groups.

Although the reliability of this quantitative analysis of the epoxy cure reaction was confirmed by previous workers (42, 43), we reconfirmed it for our system. To demonstrate the reliability, normalized peak areas in the spectra were measured with respect to the epoxide concentration. In this experiment, specimens with different epoxide concentrations were cured at high temperature for enough time to ensure complete reaction between epoxide and amine functional groups. The cure condition was 50 °C for 1 h followed by 80 °C for 2 h and 125 °C for 3 h. Formulations were smeared onto KBr IR disposable cards for the samples with pure DGEBA and those with a lower amine ratio because they did not solidify after the cure. The other samples were prepared by casting thin films with a 0.5 mm thickness using glass plates and Teflon spacers. As shown in Figure 3a, the normalized absorbances decrease linearly as epoxide concentration decreases, which indicates that our analysis is reliable and obeys the Beer−Lambert law.

To estimate the amount of absorbed water for each exposure condition, the normalized area of the characteristic water peak around 5230 $cm^{-1}$ was obtained, which has been assigned to a combination of asymmetric stretching ($\upsilon_{as}$) and in-plane deformation ($\delta$) of water (44–46). The normalized area of the characteristic water peak is known to be a way to measure the amount of absorbed water in various polymer-water systems, where the normalized area is proportional to the real amount of absorbed water (44–47). In this work, the region from 4972 to 5342 $cm^{-1}$ was taken to measure the area and normalized by the phenyl absorbance at 4622 $cm^{-1}$. Because these are normalized values we can not use them to determine absolute concentrations of water present; however, because the normalized areas are proportional to the amount of water they can be used for relative comparisons. It is also important to note that this peak includes hydroxyl groups generated in the epoxy network due to the cure reaction. To check the contribution of these hydroxyl groups to the total absorbance, we made measurements for both exposed and unexposed samples over a range of conversions. As shown in Figure 3b, for the range of epoxide conversion between 0.86 and 1.00, the absorbance due to the hydroxyl groups is approximately constant, indicating that the change in absorbance of this peak is due to the change in amount of absorbed water.

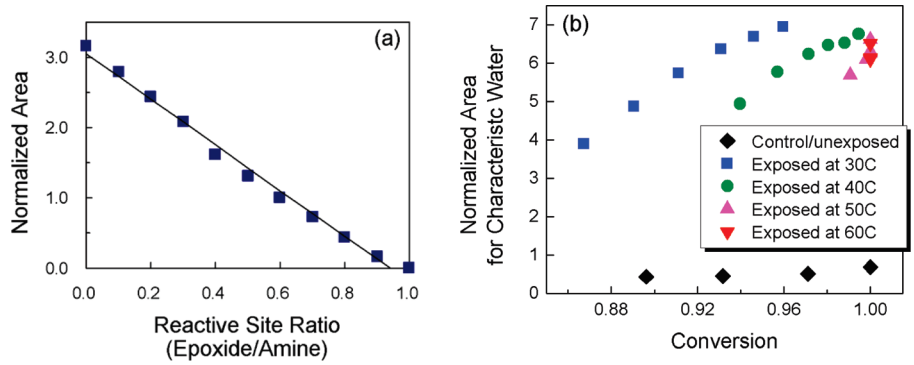


**FIGURE 3. Experimental confirmation of reliability of quantitative analyses from FTIR. (a) Plot of normalized area assigned to epoxide at 4530 $cm^{-1}$ with variation in epoxide/amine ratio. The correlation coefficient value, $R^2$ is 0.99. (b) Normalized area for characteristic water peak around 5230 $cm^{-1}$ for various unexposed and exposed systems.**

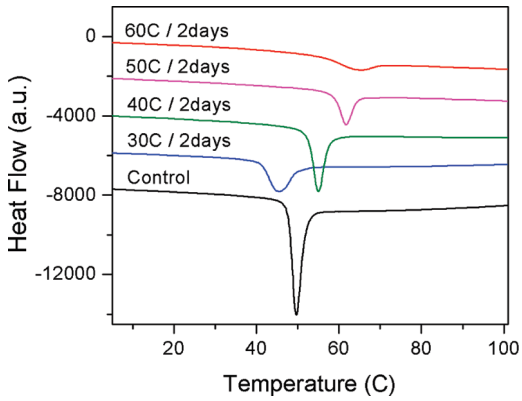


**FIGURE 4. Typical DSC curves after water immersion for 2 days at different temperatures compared with no exposure.**

## RESULTS

Our results, shown in Figure 4, clearly indicate that "anomalous" behavior, defined as an increase in glass transition after exposure to water, occurs. As shown in Figure 4, exposure to 40, 50, and 60 °C water for 2 days results in significant increases in $T_g$ as compared to the control specimen that was measured before the exposure was started. On the contrary, when the specimens were exposed to 30 °C water for 2 days, they showed a lower $T_g$ than the control.

From Figure 5 showing the entire DSC scans for each exposed system, it is shown that endothermic aging peaks are superimposed around the glass-transition region. Amorphous polymers, which are cooled down to below $T_g$ or isothermally cured at a temperature below $T_g$, typically show enthalpy relaxation upon reheating, which is observed as an endothermic peak in the DSC scan. This behavior is well-known as a structural enthalpy relaxation or physical aging, and is a result of the recovery of enthalpy trapped in the glassy state of the material during aging (48–53). Figure 5 shows that the intensity of the endothermic peaks rapidly decreased upon exposure at 60 °C, which is attributed to the fact that the exposure temperature is above $T_g$ of the system, leading the system closer to thermodynamic equilibrium as exposure continues (48, 49).

To follow the changes in $T_g$ for each exposure condition, we measured $T_g$ as a function of time for each exposure condition. As shown in Figure 6, samples exposed at 40 and 50 °C show continuous increases in $T_g$ with exposure until the rates of increase slow down and approach saturation points. Exposures at 30 and 60 °C show some interesting results that are contrary to each other. For samples exposed at 30 °C, an initial decrease in $T_g$ was followed by an increase, whereas samples exposed at 60 °C showed an increase in $T_g$ at the beginning stage, but a slight decrease in $T_g$ at the later stage of exposure.

To examine the mechanisms of this anomalous "property gain", changes in conversion were investigated using NIR spectroscopy. Typical NIR spectra are displayed in Figure 7a, in which samples exposed to water immersion for 1 day at different temperatures are compared with control samples which had been exposed to air for 1 day. The cure condition was the same as used for measuring changes in $T_g$, namely, 4 weeks at room temperature in air before the exposure was started. As shown in Figure 7a, the area of the epoxide peak around 4530 $cm^{-1}$ decreased after hygrothermal exposure compared with the control, indicating a post-curing reaction occurred during the exposure that resulted in an increase in conversion.

To follow the changes in conversion for each exposure condition, we measured conversion as a function of time for each exposure condition. Figure 7b shows that the epoxide conversion increased for all the exposure conditions, resulting in significant increases in cross-link density compared with the unexposed sample. This result shows that the elevated temperature of the water caused additional cure, even at a low temperature such as 30 °C.

When this figure is compared to the changes in $T_g$ with hygrothermal exposure in Figure 6, it is obvious that the increase in cross-link density leads to the "anomalous" increase in $T_g$ with hygrothermal exposure. Careful comparison of Figures 6 and 7b also shows that the hygrothermal behavior is complex. For example, the samples exposed at 30 °C showed an initial decrease in $T_g$, and samples exposed at 60 °C showed a decrease in $T_g$ at the latter stages of exposure, even though the conversion is continuously increasing with exposure. Thus, we can conclude that plasticization also plays a significant role in determining the properties of this system.

## DISCUSSION

For the epoxy system being examined in this study, hygrothermal exposure induces complex behavior in which an increase in glass transition due to increasing cure simultaneously occurs with a decrease in glass transition due to plasticization. From the comparison of the two figures showing changes in $T_g$ and conversion with hygrothermal exposure (Figures 6 and 7b), we can see that the increase in $T_g$ due to additional cure and the decrease in $T_g$ due to plasticization are in competition with each other during exposure.

When observing the initial stage of the sample exposure between 0 and 1 day at 30°C, plasticization has the predominant effect on $T_g$, compared with additional cure, causing a decrease in $T_g$ despite an increase in cross-link density. However, as exposure continues, the additional cure becomes the dominating factor, resulting in an increase in $T_g$. On the contrary, for exposure at 60 °C, a continuous increase in $T_g$ at the initial stage of the exposure indicates that additional cure dominates the change in $T_g$. The effect of plasticization becomes more important at the later stage of exposure, resulting in a slight decrease in $T_g$. With regards to exposure at 40 and 50 °C, it is observed that the increase in cross-link density is dominant throughout the exposure, resulting in a monotonic increase in $T_g$. When comparing samples at 50 and 60 °C, the $T_g$ for 50 °C samples is larger than $T_g$ for 60 °C samples after 8 days exposure even though both had already reached 100% conversion, which indicates that at 60 °C there is more absorbed water, resulting in greater plasticization.

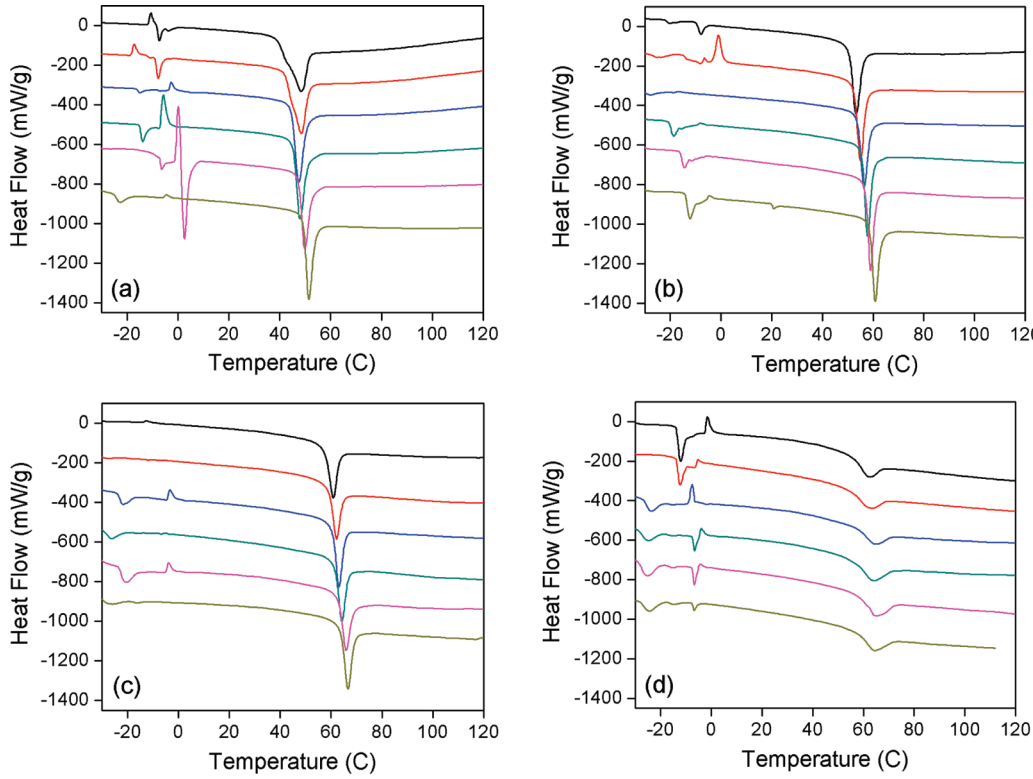


FIGURE 5. Changes in DSC curves as a function of immersion time for each exposure condition. From top of each set of DSC scans: Exposed for 1, 2, 4, 7, 14, and 28 days. Exposed in (a) 30, (b) 40, (c) 50, and (d) 60 °C water.

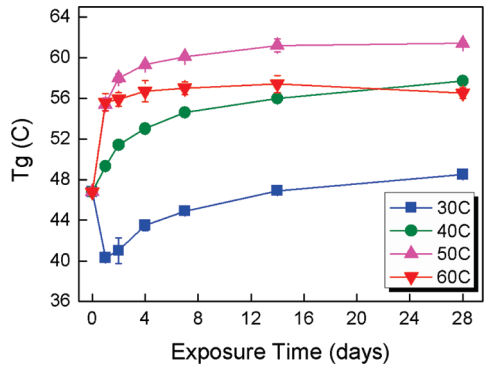


FIGURE 6. Changes in $T_g$ after water immersion at different temperatures. Samples were cured for 4 weeks at room temperature in air before exposure was started. In this picture, the size of the error bars displaying the standard deviation is too small to be shown at some points.

As described previously, two other factors that have been hypothesized to cause this "anomalous" behavior are creation of a hydrogen-bonded network of water and the influence of the epoxy microstructure. To determine the relative importance of these effects, $T_g$ for the unexposed system was plotted as a function of conversion. This "master plot" can then be used to exclude the influence of crosslink density by plotting the results from Figures 6 and 7b onto this "master plot", which makes it possible to compare the $T_g$ values directly between exposed and unexposed systems at the same conversion value.

Cross-link density is known to be one of the important factors to determine the $T_g$ in network polymers. An increase in the cross-link density reduces the chain mobility resulting in an increase in $T_g$, whereas an increase in molecular weight as well as a decrease in low-molecular-weight components during the curing reaction also increases the $T_g$ (54). The relationship between $T_g$ of a network polymer and conversion is well-described elsewhere (55–57). For derivation of the relationship, a thermodynamic theory is used in which changes in heat capacity of each component and its $T_g$ are correlated to describe the glass transition in copolymer systems. The theory was then developed into the following semiempirical equation to describe $T_g$ in cross-linked systems with the variation in conversion, assuming $\Delta C_p$ is inversely proportional to temperature

$$T_g = \frac{(1-\alpha)T_{g0} + \alpha(\Delta C_{p\infty}/\Delta C_{p0})T_{g\infty}}{(1-\alpha) + (\Delta C_{p\infty}/\Delta C_{p0})\alpha} \quad (1)$$

where α is conversion, $T_{g0}$ and $T_{g\infty}$ are the $T_g$ values of the monomer and the fully cured network, and $\Delta C_{p0}$ and $\Delta C_{p\infty}$ are the heat capacity changes at $T_{g0}$ and $T_{g\infty}$, respectively.

Using a similar approach assuming $\Delta C_p$ is constant, another semiempirical equation can be derived as shown below

$$\ln(T_g) = \frac{(1-\alpha)\ln(T_{g0}) + (\Delta C_{p\infty}/\Delta C_{p0})\alpha\ln(T_{g\infty})}{(1-\alpha) + (\Delta C_{p\infty}/\Delta C_{p0})\alpha} \quad (2)$$

To construct the master plot of $T_g$ as a function of conversion, $T_g$ and conversion values under identical cure conditions were experimentally obtained for the unexposed

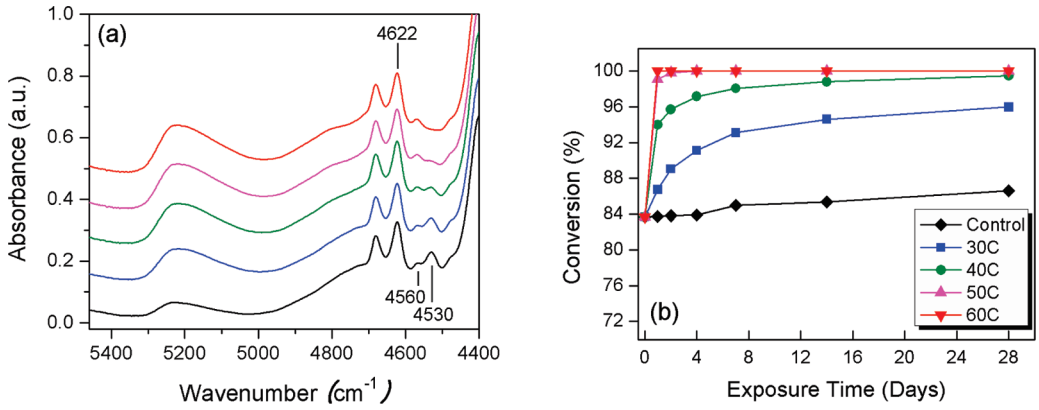


FIGURE 7. (a) Near-infrared spectra for samples immersed in water for 1 day at different temperatures compared with an unexposed control sample. Cure condition was 4 weeks at room temperature in air before the exposure was started. (b) Changes in conversion at different exposure conditions after curing 4 weeks at room temperature in air.

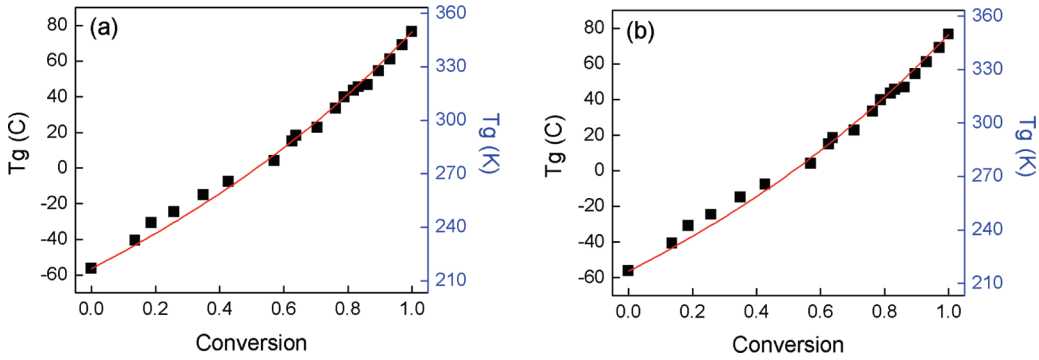


FIGURE 8. $T_g$ versus conversion "master plot" for unexposed epoxy. Points were experimentally obtained and solid line are fits to theoretical (a) eq 1 and (b) eq 2.

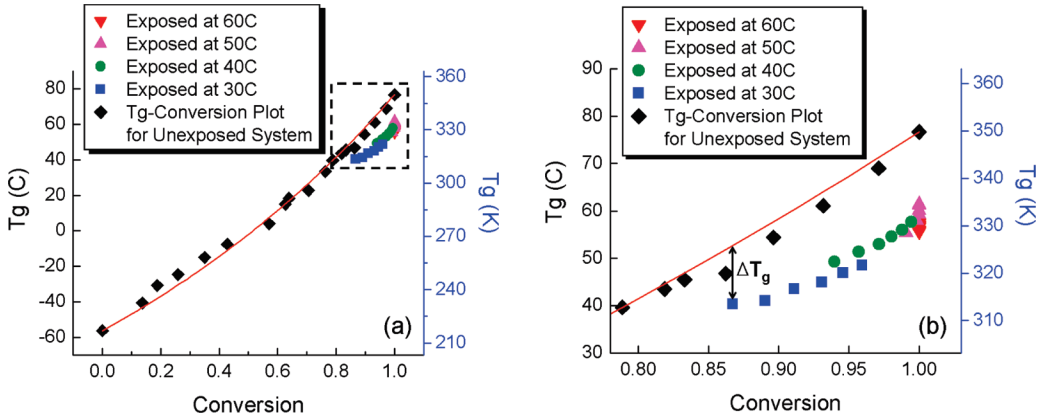


FIGURE 9. Direct comparison of $T_g$ between unexposed and exposed systems using the master plot of $T_g$ versus conversion. The section marked with dotted lines in (a) is magnified in (b).

system. Equations 1 and 2 were used for fitting the experimentally obtained data as shown in Figure 8. Both equations have good agreement to the experimental data, with coefficients of determination of 0.99 for both cases. The values of $\Delta C_{p\infty}/\Delta C_{p0}$ as a fitting parameter were 0.69 and 0.88 for eqs 1 and 2, respectively.

Finally, the values of $T_g$ and conversion for exposed systems, shown in Figures 6 and 7b, were applied to the master plots using eq 2 for the fitting. As shown in Figure 9, all the $T_g$ points for the exposed systems are below the line, showing the effect of plasticization independent of crosslink density. This result also suggests that the contribution of other factors suggested to cause "property gain", such as different types of hydrogen bonded water and the influence of microstructure are small compared to plasticization.

To further evaluate the plasticization effect quantitatively, we determined $\Delta T_g$, the difference in $T_g$ between unexposed and exposed samples at the same conversion value. Glass-transition temperatures for the exposed system were determined directly from DSC measurements, whereas $T_g$ values at the corresponding conversion for the unexposed system were obtained from the values on the fitted curve as indicated in Figure 9b. Finally, to correlate $\Delta T_g$ with the absorbed water amount at each exposure condition, the relative amount of water uptake was determined from the

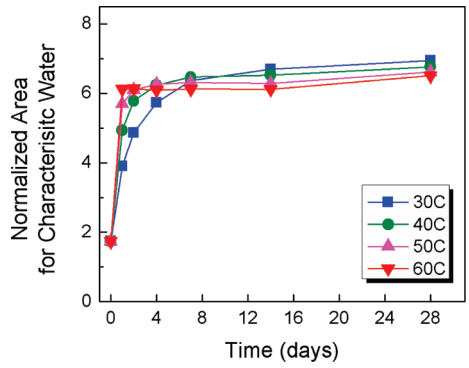


**FIGURE 10. Relative amount of water absorption with exposure time estimated by normalized area of the characteristic water peak from NIR.**

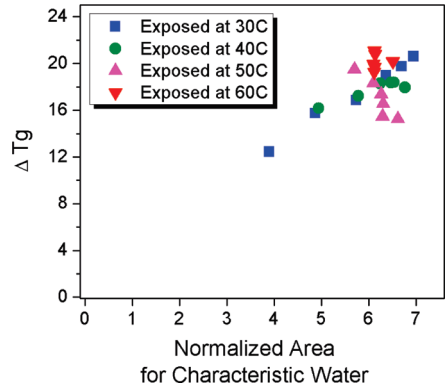


**FIGURE 11. $T_g$ differences between unexposed and exposed systems as a function of estimated amount of absorbed water.**

characteristic water peak around 5230 $cm^{-1}$, which was well-resolved in the NIR spectra of this system.

When the relative amount of absorbed water is evaluated by this method, it shows the typical features of water uptake with exposure time in which water amount increases as exposure continues, ultimately approaching some saturation point, as shown in Figure 10. The rate of increase in absorbed water at the initial stage of the exposure is enhanced as exposure temperature increases, which is also a typical feature in that water absorption of the epoxy system is accelerated with an increase in diffusion rate as temperature increases.

Finally, $\Delta T_g$ was plotted as a function of the relative absorbed water amount for each exposure condition (Figure 11). For samples exposed at 30 and 40 °C, $\Delta T_g$ increases with water amount, showing the expected behavior of increase in plasticization as the amount of absorbed water increases. However, for the 50 and 60° C samples, some anomalous behavior is observed in which $\Delta T_g$ changes independently of water content. This anomalous behavior possibly indicates that there are other factors affecting "property gain" such as secondary types of hydrogen-bonded water and microstructure, although these effects are very small compared with plasticization.

## CONCLUSIONS

For the anomalous hygrothermal behavior of an epoxy-amine thermoset, in which $T_g$ increased with exposure to water immersion at different temperatures, FT-NIR spectroscopic studies demonstrated that increases in cross-link density due to additional cure during the elevated temperature exposure led to an increase in properties. However, from the feature that the $T_g$ decreased at certain stages of the exposure, it is evident that plasticization by water occurred simultaneously, rendering the hygrothermal behavior to be more complex than originally hypothesized. In this complex hygrothermal behavior, "property gain" by an increase in cross-link density and "property loss" by plasticization occurred simultaneously.

Constructing the plot of $T_g$ versus conversion for the unexposed system provided an excellent method to consider contributions of other factors and exclude the factor of crosslink density. By applying the results for the exposed system onto this "master plot", it is possible to directly compare the $T_g$ values between exposed and unexposed samples while ruling out the factor of cross-link density. The result indicates that the effect of other factors, such as different types of hydrogen-bonded water and influence of the microstructure, are very small compared to the plasticization effect.

To evaluate the plasticization effect quantitatively, we measured $\Delta T_g$, the difference of $T_g$ between unexposed and exposed samples at the same conversion value, as a function of absorbed water amount. It is observed that $\Delta T_g$ increases with absorbed water amount at lower exposure temperatures, whereas $\Delta T_g$ changes independently of water amount at higher exposure temperatures. Thus, factors other than additional cure and plasticization may affect $T_g$ at these higher exposure temperatures. Examination of these other factors such as changes in the relative amounts of the hard and soft phases and different states of hydrogen-bonded water molecules are currently ongoing in order to provide an in-depth understanding of the anomalous behavior in this system.

**Acknowledgment.** This work is supported by National Science Foundation Grant CMS-0653969.

## REFERENCES AND NOTES

(1) Sung, Y. K.; Gregonis, D. E.; Russell, G. A.; Andrade, J. D. *Polymer* **1978**, *19*, 1362–1363.
(2) Oksanen, C. A.; Zografi, G. *Pharm. Res.* **1993**, *10*, 791–799.
(3) Tan, Y. Y.; Challa, G. *Polymer* **1976**, *17*, 739–740.
(4) Lassila, L. V. J.; Nohrstrom, T.; Vallittu, P. K. *Biomaterials* **2002**, *23*, 2221–2229.
(5) Jin, X.; Ellis, T. S.; Karasz, F. E. *J. Polym. Sci., Part B: Polym. Phys.* **1984**, *22*, 1701–1717.
(6) Hodge, R. M.; Bastow, T. J.; Edward, G. H.; Simon, G. P.; Hill, A. J. *Macromolecules* **1996**, *29*, 8137–8143.
(7) Birkinshaw, C.; Buggy, M.; Daly, S. *Polym. Commun.* **1987**, *28*, 286–288.
(8) Ellis, T. S.; Karasz, F. E. *Polymer* **1984**, *25*, 664–669.
(9) McKague, E. L.; Reynolds, J. D.; Halkias, J. E. *J. Appl. Polym. Sci.* **1978**, *22*, 1643–1654.
(10) Lagaron, J. M.; Powell, A. K.; Bonner, G. *Polym. Test* **2001**, *20*, 569–577.
(11) Pissis, P.; Apekis, L.; Christodoulides, C.; Niaounakis, M.; Kyritsis, A.; Nedbal, J. *J. Polym. Sci., Part B: Polym. Phys.* **1996**, *34*, 1529–1539.
(12) Deneve, B.; Shanahan, M. E. R. *Polymer* **1993**, *34*, 5099–5105.
(13) Xiao, G. Z.; Delamar, M.; Shanahan, M. E. R. *J. Appl. Polym. Sci.* **1997**, *65*, 449–458.

(14) Xiao, G. Z.; Shanahan, M. E. R. *J. Appl. Polym. Sci.* **1998**, *69*, 363–369.
(15) Moy, P.; Karasz, F. E. *Polym. Eng. Sci.* **1980**, *20*, 315–319.
(16) Carter, H. G.; Kibler, K. G. *J. Compos. Mater.* **1977**, *11*, 265–275.
(17) Jelinski, L. W.; Dumais, J. J.; Cholli, A. L.; Ellis, T. S.; Karasz, F. E. *Macromolecules* **1985**, *18*, 1091–1095.
(18) Perrin, F. X.; Nguyen, M. H.; Vernet, J. L. *Eur. Polym. J.* **2009**, *45*, 1524–1534.
(19) LaPlante, G.; Lee-Sullivan, P. *J Appl. Polym. Sci.* **2005**, *95*, 1285–1294.
(20) Theocaris, P. S.; Kontou, E. A.; Papanicolau, G. C. *Colloid Polym. Sci.* **1983**, *261*, 394–403.
(21) Nunez, L.; Villanueva, M.; Fraga, F.; Nunez, M. R. *J. Appl. Polym. Sci.* **1999**, *74*, 353–358.
(22) Apicella, A.; Nicolais, L. *Adv. Polym. Sci.* **1985**, *72*, 69–77.
(23) Yang, Q.; Xian, G.; Karbhari, V. M. *J Appl. Polym. Sci.* **2008**, *107*, 2607–2617.
(24) Lu, M. G.; Shim, M. J.; Km, S. W. *J Appl. Polym. Sci.* **2001**, *81*, 2253–2259.
(25) Nogueira, P.; Ramirez, C.; Torres, A.; Abad, M.; Cano, J.; Lopez, J.; Lopez-Bueno, I.; Barral, L. *J. Appl. Polym. Sci.* **2001**, *80*, 71–80.
(26) Lobanov, Y. E.; Shterenzon, A. L. *Mech. Compos. Mater.* **1971**, *7*, 654–656.
(27) Zhou, J.; Lucas, J. P. *Polymer* **1999**, *40*, 5505–5512.
(28) Gupta, V. B.; Drzal, L. T.; Rich, M. J. *J. Appl. Polym. Sci.* **1985**, *30*, 4467–4493.
(29) Maggana, C.; Pissis, P. *J. Polym. Sci., Part B: Polym. Phys.* **1999**, *37*, 1165–1182.
(30) Vanlandingham, M. R.; Eduljee, R. F.; Gillespie, J. W. *J. Appl. Polym. Sci.* **1999**, *71*, 787–798.
(31) Bellenger, V.; Verdu, J.; Morel, E. *J. Mater. Sci.* **1989**, *24*, 63–68.
(32) Grave, C.; McEwan, I.; Pethrick, R. A. *J. Appl. Polym. Sci.* **1998**, *69*, 2369–2376.
(33) Adamson, M. J. *J. Mater. Sci.* **1980**, *15*, 1736–1745.
(34) Mikols, W. J.; Seferis, J. C.; Appicella, A.; Nicolais, L. *Polym. Compos.* **1982**, *3*, 118–124.
(35) Wu, L.; Hoa, S. V.; Minh-Tan; Ton-That, *J Appl. Polym. Sci.* **2006**, *99*, 580–588.
(36) Devasahayam, S. *J Appl. Polym. Sci.* **2006**, *99*, 3318–3327.
(37) Thomson, K. W.; Wong, T.; Broutman, L. J. *Polym. Eng. Sci.* **1984**, *24*, 1270–1276.
(38) Netravali, A. N.; Fornes, R. E.; Gilbert, R. D.; Memory, J. D. *J Appl. Polym. Sci.* **1985**, *30*, 1573–1578.
(39) Johncock, P. *J Appl. Polym. Sci.* **1990**, *41*, 613–618.
(40) Zhou, J.; Lucas, J. P. *Polymer* **1999**, *40*, 5513–5522.
(41) Papanicolaou, G. C.; Komidou, Th. V.; Vatalis, A. S.; Delides, C. G. *J Appl. Polym. Sci.* **2006**, *99*, 1328–1339.
(42) Dannenberg, H. *SPE Trans.* **1963**, *3*, 78–88.
(43) Chike, K. E.; Myrick, M. L.; Lyon, R. E.; Angel, S. M. *Appl. Spectrosc.* **1993**, *47*, 1631–1635.
(44) Musto, P.; Ragosta, G.; Mascia, L. *Chem. Mater.* **2000**, *12*, 1331–1341.
(45) Musto, P.; Ragosta, G.; Scarinzi, G.; Mascia, L. *J. Polym. Sci., Part B: Polym. Phys.* **2002**, *40*, 922–938.
(46) Musto, P.; Mascia, L.; Ragosta, G.; Scarinzia, G.; Villano, P. *Polymer* **2000**, *41*, 565–574.
(47) Fukuda, M.; Kawai, H.; Yagi, N.; Kimura, O.; Ohta, T. *Polymer* **1990**, *31*, 295–302.
(48) Fraga, F.; Castro-Diaz, C.; Rodriguez-Nunez, E.; Martinez-Ageitos, J. M. *Polymer* **2003**, *44*, 5779–5784.
(49) Ribas, S. M. *Progr. Colloid Polym.* **1992**, *87*, 78–82.
(50) Shi, X.; Fernando, B. M. D.; Croll, S. G. *J. Coat. Technol. Res.* **2008**, *5*, 299–309.
(51) Bockenheimer, C.; Fata, D.; Possart, W. *J. Appl. Polym. Sci.* **2004**, *91*, 369–377.
(52) Montserrat, S.; Cortes, P.; Calventus, Y.; Hutchinson, J. M. *J. Therm. Anal.* **1997**, *49*, 79–85.
(53) Fraga, F.; Payo, P.; Rodriguez-Nunez, E.; Martinez-Ageitos, J. M.; Castro-Diaz, C. *J. Appl. Polym. Sci.* **2006**, *103*, 3931–3935.
(54) Venditti, R. A.; Gillham, J. K. *Polym. Mater. Sci. Eng.* **1993**, *69*, 434.
(55) Wise, C. W.; Cook, W. D.; Goodwin, A. A. *Polymer* **1997**, *38*, 3251–3261.
(56) Couchman, P. R.; Karasz, F. E. *Macromolecules* **1978**, *11*, 117–119.
(57) Pascault, J. P.; Williams, R. J. J. *J. Polym. Sci., Part B: Polym. Phys.* **1990**, *28*, 85–95.

AM9009346